



Theoretical model for surface diffusion driven Ni-particle agglomeration in anode of solid oxide fuel cell



Sheng Gao^a, Jiayu Li^a, Zijing Lin^{a,b,*}

^a Hefei National Laboratory for Physical Sciences at Microscale, Department of Physics, University of Science and Technology of China, Hefei 230026, China

^b Key Laboratory of Materials Physics, Institute of Solid State Physics, Chinese Academy of Sciences, Hefei 230031, China

HIGHLIGHTS

- An analytical model capable of explaining experiments is derived in a natural way.
- Mechanism and limiting factor for Ni particle growth are discussed and quantified.
- Only one adjustable parameter describing electrode morphology is used in the model.
- The model is in very good agreements with the available experimental data sets.

ARTICLE INFO

Article history:

Received 2 July 2013

Received in revised form

27 December 2013

Accepted 8 January 2014

Available online 15 January 2014

Keywords:

Coarsening

Growth kinetics

Random packing

Connectivity

Coordination number

Solid oxide fuel cell

ABSTRACT

The agglomeration of Ni particles in nickel–yttria stabilized zirconia (YSZ) anode is an important degradation mechanism for the solid oxide fuel cell and is widely believed to be driven by surface diffusion. This work aims to develop a quantitative model to describe the agglomeration kinetics. The model treats the anode as a system of random packing Ni and YSZ particles. Surface diffusion occurs between the connected Ni particles of different sizes characterized by two representative radii, but is influenced by the YSZ network. The Fick's law for diffusion, the Gibbs–Thomson relation for vacancy concentration and the coordination number theory for percolating Ni network are employed in the mathematical derivation. The growth kinetics is expressed as an analytical function consisting of two model parameters, one for the Ni-particle size distribution and the other for the influence of the YSZ backbone. The model is in excellent agreement with the available experiments. The influence of the YSZ backbone is further considered to obtain a model with just one fitting parameter. The one-parameter model is also in good agreement with the experiments and the fundamental physics for the Ni-particle growth is therefore believed to be well characterized.

© 2014 Elsevier B.V. All rights reserved.

1. Introduction

Reliability and long-term stability are crucial for solid oxide fuel cell (SOFC) to become a commercially mature energy conversion technology. Research on the mechanisms responsible for the performance degradation is receiving increased attention in recent years. Degradation occurs for all SOFC components and for a variety of reasons. For example, crack formation and loss of ionic conductivity in the electrolyte [1–6], increase of the contact resistance between electrodes and current collectors [7–15], reactions between electrolyte and electrode materials and densification of the

electrode structure [16,17], coarsening of electrode particles [18–28], delamination between electrode and electrolyte [7,29–31] and the Cr poisoning of the cathode [32–34], etc. Among the degradation phenomena observed, the agglomeration of Ni-particles in anode of SOFC has received particular attention as the porous Ni–YSZ cermet is the most widely used anode material and the agglomeration process that results in decreasing electrochemical performance may occur in a relatively short period of time [18–21,25–28]. Due to the complexity of the agglomeration phenomena and their underlying mechanisms, the progress in the development of theoretical models to describe the kinetics of this process is rather limited.

The agglomeration of Ni-particles is strongly affected by the contents of YSZ and water vapor. The presence of YSZ limits the space for the growth of the Ni particles [21,26]. The water vapor accelerates the agglomeration process, though its effect on the final

* Corresponding author. Key Laboratory of Materials Physics, Institute of Solid State Physics, Chinese Academy of Sciences, Hefei 230031, China. Tel.: +86 551 63606345; fax: +86 551 63606348.

E-mail address: zjlin@ustc.edu.cn (Z. Lin).

grain size of Ni particles may be limited [8,35]. The mechanism for the influence of water vapor on the agglomeration process is complicated and is conjectured to be due to its role in changing the partial pressure of Ni gas species [35] and the surface diffusion coefficient of Ni atoms [36], etc. To avoid the ambiguity caused by the yet to be understood role of water vapor, the existing models focus on describing the growth of Ni particles working under low water vapor pressure. A general feature of these models [19,26,27,35,37,38] is to augment the traditional theory for the agglomeration of particles with some empirical function to account for the observed asymptotic behavior of Ni particle growth. For example, Vaßen et al. [26] developed a theory for the growth of Ni particles with the surface diffusion as the dominant mechanism, but had to arbitrarily introduce a limiting function to mimic the asymptotic feature of the Ni particle growth. Even though the theory may fit well with their own experimental data, the deduced surface diffusion coefficient of Ni is 2–3 orders of magnitude smaller than the literature data. Similar limiting function was also used empirically by Nakajo et al. [38] in their modeling of the coarsening of Ni particles. Naturally, it is desirable to avoid enforcing the experimentally observed asymptotic feature in the theoretical model by arbitrarily introducing some empirical function. Recently, Chen et al. applied a phase-field approach to simulate the microstructural evolution of Ni–YSZ anode in terms of the triple phase boundary (TPB) density [27]. Even though such simulation eliminates the use of the empirical limiting function, it lacks the transparency possessed by an analytical model. Moreover, it is nontrivial to compare the simulation results with the experimental observations. For example, the presented simulation results for the chosen modeling parameters indicate much faster agglomeration processes than typically observed experimentally.

This work focuses on developing a coherent theoretical model for the agglomeration of Ni-particles in SOFC anode. The model in this paper builds on the foundation of significant earlier literature. The model uses the surface diffusion as the dominant agglomeration mechanism and incorporates the concept of coordination number in the percolation theory and the statistical nature of the random packing of Ni–YSZ particles in the anode. The resulting theory is in a simple analytical form with two adjustable parameters and fits the experiments well. The two parameters are further reduced to one based on reasonable physical consideration. The model with only one adjustable parameter is also shown to fit the experiments very well.

2. Theory

The agglomeration of Ni particles in Ni–YSZ cermet is in principle a capillarity-driven phenomenon. The growth of Ni grains may take place through different mechanisms: evaporation–condensation, bulk diffusion and surface diffusion. The evaporation–condensation mechanism is negligible as the vapor pressure of Ni-containing species is very low at the typical SOFC operating conditions ($T < 1000^\circ\text{C}$) [35]. The grain boundary or bulk diffusion is estimated to be 3 orders of magnitude smaller than the surface diffusion [27]. Therefore, it is reasonable to consider the surface diffusion as the only driving mechanism.

The mass transport via the surface diffusion takes place between Ni particles of different curvatures. The larger Ni particles grow at the expense of the smaller ones which may tend to disappear, as schematically illustrated in Fig. 1a. To capture the essence of the physical process in simple terms, the complicated geometry of Ni particles in a Ni–YSZ cermet is modeled as a system of two sets of spherical Ni particles, with radii of r_l and r_s for the large and small particles, respectively. Due to the difference in the vacancy concentrations of the large and small particles, there is a

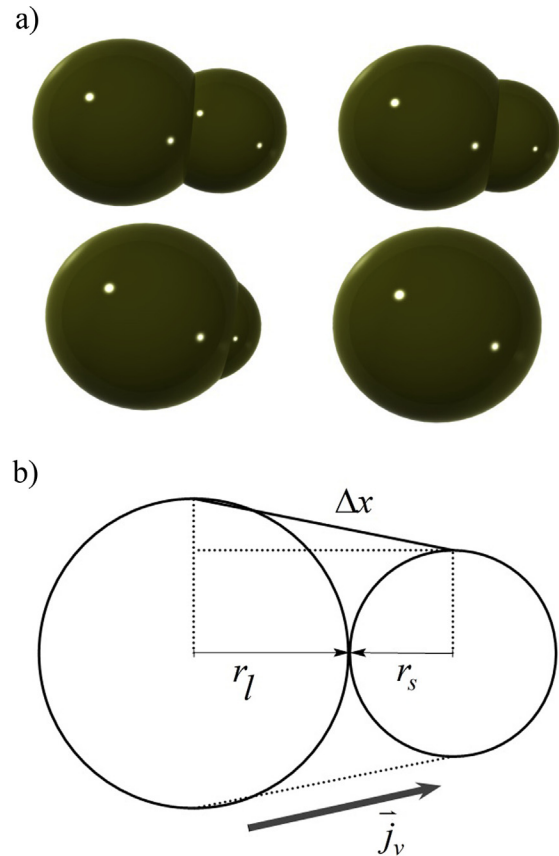


Fig. 1. Schematic of the agglomeration of Ni-particle: a) the process of coarsening, b) geometric model of the two-particle system.

thermodynamically-driven diffusion of vacancy from the large particle to the small one (Fig. 1b). Or equivalently, the Ni atoms diffuse from the small particle to the large one. As a result, the size of the large particle grows while the small particle gets smaller.

The rate of volumetric change of the large particle should be equal to the total volumetric flow diffused from nearby particles:

$$\frac{dV_l}{dt} = 4\pi r_l^2 \frac{dr_l}{dt} = \sum |\nu_f| = n j_v \Delta S \Omega \quad (1)$$

where V_l is the volume of the large Ni particle, t is the time, ν_f is the volumetric flow between the large and small Ni particles, n is the number of Ni particles connected to the large particle for the diffusion to take place, j_v is the magnitude of vacancy flow between a contacting pair of large and small particles, ΔS is the surface diffusion area of the vacancy flow, Ω is the diffusion volume element that is often reasonably approximated by the atomic volume of Ni (10.9 \AA^3).

For the convenience of evaluating the quantities in Eq. (1) and connecting the theoretical model with the experiment, it is helpful to use the mean particle radius, $r_m = (r_l + r_s)/2$, and introduce a proportionality parameter $\beta = (r_l - r_s)/2r_m$ regarding the particle radius difference. Following Vaßen et al. [26], β is assumed to be constant during the agglomeration process. The assumption may be empirically justified by the fact that the average particle radius difference is generally large when the average particle size is large. However, it should be pointed out that β by itself is only a phenomenological parameter like r_l or r_s . They are used to simplify the kinetic model and should not be interpreted too literally. The final test of the model rests on the comparison of the theoretical and experimental results on the Ni particle growth, $r_m = r_m(t)$.

In terms of r_m and β , one has $r_l = (1 + \beta)r_m$ and $r_s = (1 - \beta)r_m$. Eq. (1) may be rewritten as,

$$4\pi(1 + \beta)^3 r_m^2 \frac{dr_m}{dt} = n j_v \Delta S \Omega. \quad (2)$$

Based on a random packing of Ni–YSZ spheres, the average number of small particles connected to one large particle may be expressed as:

$$n = k_{YSZ} \frac{Z_{Ni,Ni}}{2}, \quad (3)$$

where $Z_{Ni,Ni}$ is the coordination number between Ni particles, i.e., the average number of contacts between Ni particles [39]. $Z_{Ni,Ni}$ is divided by 2 because only the contacted small particles contribute to the diffusion flow. k_{YSZ} is used to account for the blocking effect of the YSZ backbone on the Ni particle growth.

During the process of Ni particle growth, the YSZ particles are known to remain essentially intact due to the very high melting temperature of the YSZ material [19–21]. The backbone formed by the unchanging YSZ particles provides a limited space for the Ni particle growth, as shown schematically in Fig. 2. Moreover, the YSZ backbone also affects the connectivity of the percolating network of Ni particles. The total number of Ni particles is expected to gradually decrease in the process of agglomeration. During the agglomeration, some initially percolated Ni particles may become disconnected from the percolating network, while the others remain connected, as illustrated in Fig. 2. The connected Ni particles remain active in the agglomeration process, while the disconnected Ni particles stop growing in size. That is, there is some probability for a particle to stop growing at a given time. In other words, there is a distribution of growth lifetime for the Ni particles [40]. k_{YSZ} is introduced in Eq. (3) to describe this fact and corresponds to the probability of Ni particle with a growth lifetime, T , larger than a given time, t , i.e., $k_{YSZ} = P(T > t)$.

If the probability per unit time of a Ni particle stopped growing at time t is λ that may be reasonably assumed to be constant [40], the probability of Ni particles stopped growing in a time interval $(t, t + \Delta t)$ would be:

$$P(t < T < t + \Delta t | T > t) = \lambda \cdot \Delta t, \quad (\Delta t \rightarrow 0). \quad (4)$$

Here the condition “ $T > t$ ” is required as the particles stopped growing during $(t, t + \Delta t)$ necessarily means that their lifetimes are longer than T . By nature of the conditional probability, Eq. (4) may be rewritten as:

$$\begin{aligned} \lambda &= \lim_{\Delta t \rightarrow 0} P(t < T < t + \Delta t | T > t) / \Delta t \\ &= \lim_{\Delta t \rightarrow 0} P(t < T < t + \Delta t) / P(T > t) / \Delta t \\ &= \lim_{\Delta t \rightarrow 0} \frac{P(T > t) - P(T > t + \Delta t)}{P(T > t) \Delta t} \\ &= \lim_{\Delta t \rightarrow 0} \frac{k_{YSZ}(t) - k_{YSZ}(t + \Delta t)}{k_{YSZ}(t) \Delta t} \\ &= -\frac{1}{k_{YSZ}(t)} \frac{dk_{YSZ}(t)}{dt}. \end{aligned} \quad (5)$$

Solving Eq. (5) yields:

$$k_{YSZ}(t) = e^{-\lambda t}, \quad (6)$$

where the initial condition $k_{YSZ}(t = 0) = 1$ has been used.

The coordination numbers between Ni particles and YSZ particles in the SOFC anode are respectively [39,41],

$$Z_{Ni,Ni} = \bar{Z} \frac{\eta_{Ni}}{r_m} / \left(\frac{\eta_{Ni}}{r_m} + \frac{\eta_{YSZ}}{r_{YSZ}} \right), \quad (7)$$

$$Z_{YSZ,YSZ} = \bar{Z} \frac{\eta_{YSZ}}{r_{YSZ}} / \left(\frac{\eta_{Ni}}{r_m} + \frac{\eta_{YSZ}}{r_{YSZ}} \right), \quad (8)$$

where η_{Ni} (η_{YSZ}) is the volume fraction of Ni (YSZ) based on the solid phase alone ($\eta_{Ni} + \eta_{YSZ} = 1$), \bar{Z} is the average coordination number and r_{YSZ} is the mean YSZ particle radius. As YSZ is the majority component of the anode materials in most SOFC designs and the YSZ particles are known to experience very little change over time [19–21], it is reasonable to assume that the coordination number of YSZ particles, $Z_{YSZ,YSZ}$, is a constant. Combining Eqs. (7) and (8) then gives,

$$Z_{Ni,Ni} = Z_{YSZ,YSZ} \frac{\eta_{Ni}}{\eta_{YSZ}} \frac{r_m}{r_{YSZ}} = \bar{Z}_0 \frac{\eta_{Ni}}{\eta_{Ni} + \eta_{YSZ}} \frac{r_m}{r_{m0}} = \frac{B}{r_m} \quad (9)$$

Here \bar{Z}_0 is the initial average coordination number, r_{m0} (r_{YSZ0}) is the initial mean radius of Ni (YSZ) particles and the constant B is given by:

$$B = \bar{Z}_0 \frac{\eta_{Ni}}{\eta_{Ni} + \eta_{YSZ}} \frac{r_m}{r_{m0}}. \quad (10)$$

Hence, the time evolution of the average number of small particles connected to a large particle (Eq. (3)) is given by:

$$n = e^{-\lambda t} \frac{B}{2r_m}. \quad (11)$$

The vacancy flow between Ni particles of different sizes may be determined by the Fick's law:

$$\bar{j}_v = D_{v,s} \frac{dC}{dx} \approx D_{v,s} \frac{\Delta C}{\Delta x} \quad (12)$$

where ΔC is the difference in the vacancy concentration, Δx stands for the diffusion distance and $D_{v,s}$ is the vacancy surface diffusion coefficient. According to the Gibbs–Thomson relation [42], the vacancy concentration may be expressed as:

$$C_r = C_e \exp\left(\frac{2\gamma\Omega}{k_B T r}\right) \approx C_e \left(1 + \frac{2\gamma\Omega}{k_B T r}\right) \quad (13)$$

where C_e is the vacancy concentration for a flat surface, k_B is the Boltzmann constant, T is the temperature, γ is the surface energy and r is the radius of Ni particle. The difference in the vacancy concentration is therefore given by:

$$\Delta C = C_{r_s} - C_{r_l} = C_e \frac{2\gamma\Omega}{k_B T} \left(\frac{1}{r_s} - \frac{1}{r_l} \right). \quad (14)$$

As seen in Fig. 1b, the diffusion distance may be written as:

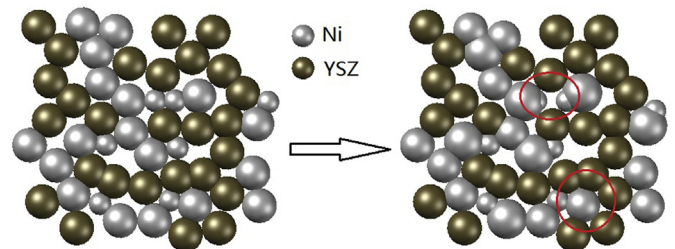


Fig. 2. The limitation on the growth space of Ni particles imposed by the YSZ backbone.

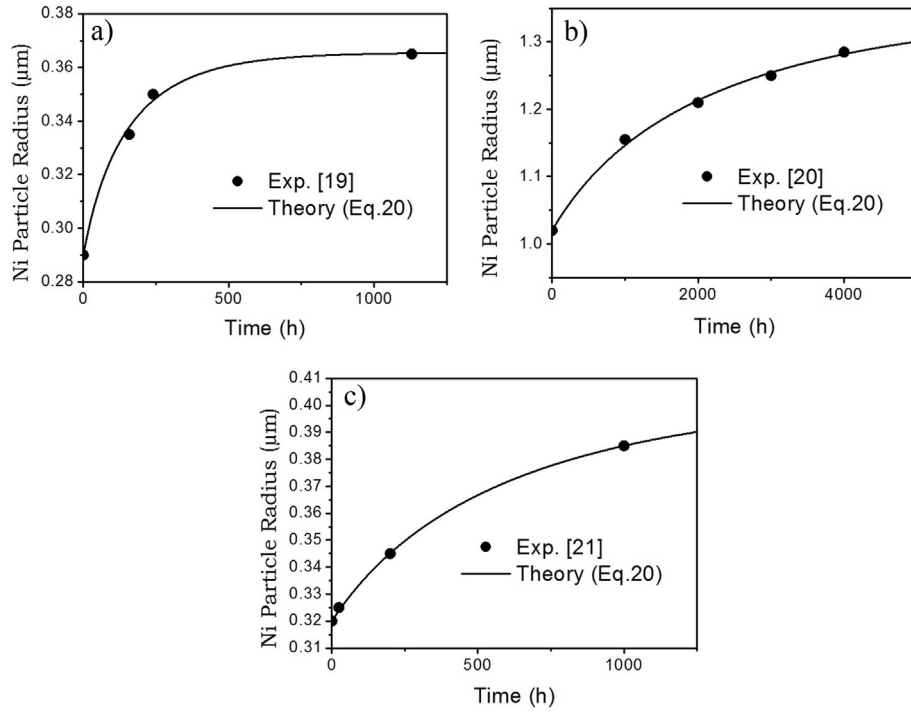


Fig. 3. Comparison of the experimental data and the theoretical fittings (Eq. (20)): a) Cell A [19], b) Cell B [20], c) Cell C [21].

$$\Delta \bar{x} = \sqrt{(r_1 + r_s)^2 + (r_1 - r_s)^2}. \quad (15)$$

Hence, the vacancy flow is given by:

$$\begin{aligned} \bar{j}_v &= D_{v,s} C_e \frac{2\gamma\Omega}{k_B T} \frac{\Delta r_m}{(r_m^2 - \Delta r_m^2)(r_m^2 + \Delta r_m^2)^{0.5}} \\ &= \frac{2\gamma D_s}{k_B T} \frac{\beta}{(1 - \beta^2)(1 + \beta^2)^{0.5} r_m^2}, \end{aligned} \quad (16)$$

where $D_s = D_{v,s} C_e \Omega$ is the atomic surface diffusion coefficient [43].

The surface diffusion area for the vacancy flow may be roughly estimated with a thickness δ_s of the inter-atomic spacing of Ni (2.5 Å) and a circumference $2\pi r_m$:

$$\Delta S = 2\pi r_m \delta_s. \quad (17)$$

With Eqs. (11), (16) and (17), Eq. (2) may be rewritten as:

$$\frac{dr_m}{dt} = C \frac{e^{-\lambda t}}{r_m^4}, \quad (18)$$

where,

$$C = D_s \frac{\gamma\Omega\delta_s}{2k_B T} \frac{\beta}{(1 - \beta^2)(1 + \beta^2)^{0.5} (1 + \beta)^3} \bar{Z}_0 \frac{\eta_{Ni}}{r_{m0}} + \frac{\eta_{YSZ}}{r_{YSZ0}}. \quad (19)$$

Solving Eq. (18) gives the time evolution of the mean particle radius of Ni as:

$$r_m = \left(\frac{5C}{\lambda} (1 - e^{-\lambda t}) + r_{m0}^5 \right)^{\frac{1}{5}}. \quad (20)$$

Eq. (20) is satisfactorily simple as it involves only two adjustable parameters, λ and C , or effectively λ and β as other quantities in C are determined by the anode composition and the properties of the Ni particles.

Before moving further on applying the model, it is helpful to be reminded with a brief discussion on the conditions for the applicability of the theory. As mentioned above, these conditions include: (1) Fuel with low water vapor content to avoid the complication caused by the effect of water vapor. Several experiments have shown that the water vapor may significantly speed up the agglomeration process via increasing the surface diffusion coefficient of Ni, but does not change the final state [8,35]. These experimental results imply the possible applicability of the model for the cases with high water vapor contents. However, that will require assumptions about the unknown effects of water vapor on the diffusion process and is not pursued here. Moreover, it is prudent not to assume the applicability of the model to the cases with high water vapor pressures as often encountered in practical operating cells. Nevertheless, the model should be directly applicable to cells with the design of gradual internal reforming where the water vapor remains at a low level throughout the cells, as demonstrated experimentally [44] and illustrated theoretically [45]; (2) Anode microstructure describable by the random packing of Ni and YSZ particles. Fortunately, the random packing model is known to describe most Ni–YSZ composite anodes well, as repeatedly demonstrated in its long history of successful applications [39,46–51]. However, revision may be required for application to some new anode designs such as the nano-composite anode with the core–shell structure [52] and the Ni nanoparticle infiltrated anode [53], as illustrated by their new electrical conductivity properties [51–53]; (3) The formation of a stable YSZ backbone. The YSZ content should be sufficiently high, say, over 35vol%, to form a highly percolated YSZ network in a conventional Ni–YSZ composite electrode [39]. If the YSZ content is low, a significant number of YSZ particles isolated by surrounding Ni particles may change their locations in the process of Ni agglomeration. In such cases, both the role of YSZ on limiting the Ni agglomeration is diminished and the coordination number theory used in the mathematical derivation may be invalid. Fortunately, almost all Ni–YSZ anode designs meet the model requirement. As a side note, it may be worthy pointing out that YSZ may in principle be replaced by other stable ceramic materials, but the

Table 1

Experimental conditions and literature data used for validating the theoretical model for the Ni-particle growth in SOFC anodes. The model parameters, β and λ , obtained by fitting are also shown.

Name	Cell A	Cell B	Cell C
Temperature T (K) [19–21]	1123.15	1273.15	1073.15
Volume fraction of Ni η_{Ni} [19–21]	0.39	0.4	0.39
Volume fraction of YSZ η_{YSZ} [19–21]	0.61	0.6	0.61
Initial radius of Ni particle r_{m0} (μm) [19–21]	0.29	1.02	0.32
Initial radii of YSZ particles r_{YSZ0} (μm) [19–21]	0.265	1.0	0.3
Atomic surface diffusion coefficient D_s ($\text{m}^2 \text{h}^{-1}$) [26]	1.04×10^{-10}	6.35×10^{-10}	4.80×10^{-11}
Volume element Ω (m^3) [26]	1.09×10^{-29}	1.09×10^{-29}	1.09×10^{-29}
Surface energy γ (Jm^{-2}) [26]	1.9	1.9	1.9
Thickness δ_s (m) [26]	2.5×10^{-10}	2.5×10^{-10}	2.5×10^{-10}
Average initial coordination number \bar{Z}_0 [50]	6.7	6.7	6.7
Fitting parameter β	0.83	0.94	0.75
Fitting parameter λ (h^{-1})	4.70×10^{-3}	3.02×10^{-4}	1.17×10^{-3}
C ($\text{m}^5 \text{h}^{-1}$) (evaluated with Eq. (19))	4.21×10^{-36}	2.03×10^{-34}	1.73×10^{-36}

replacement by volatile materials such CGO that undergoes morphological change would alter the agglomeration kinetics [54] and would invalidate the model.

3. Results and discussion

3.1. Comparison with experimental results

Due to the great effort required for the long term testing, there are only a few experimental data sets available for the model to compare to. For the convenience of referencing, the experimental results by Faes et al. [19], Simwonis et al. [20] and Tanasini et al. [21] are referred below as Cell A, Cell B and Cell C, respectively.

Fig. 3 shows the comparison of the theoretical model with the experimental data. The property parameters required by the model are chosen to be as realistic as possible and summarized in Table 1. For example, the surface diffusion coefficients of Ni correspond to the newest data by Jaunet [26]. These coefficients were obtained without the water vapor effect and might moderately underestimate that for the cells tested with a small amount (3–4%) of H_2O . The underestimation may give rise to somewhat overestimated β values, as seen in Eq. (19). As shown in Fig. 3, the current model with reasonable property parameters fits the experimental data very well. The present model is clearly superior over the model by Vaßen et al. that has to rely on arbitrarily low surface diffusion coefficients (over two orders of magnitude smaller than the Jaunet values) to reproduce the measured low growth rates [26].

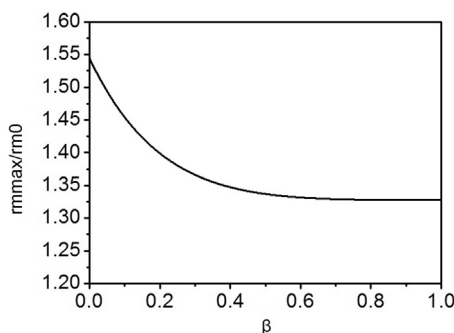


Fig. 4. Dependence of $r_{\text{mmax}}/r_{\text{m0}}$ on the model parameter β

3.2. Reduction of model parameters

Eq. (20) may be rewritten using a new pair of model parameters (β , r_{mmax}) as:

$$r_{\text{m}} = \left[(r_{\text{mmax}}^5 - r_{\text{m0}}^5) \left(1 - \exp(-\lambda(\beta, r_{\text{mmax}})t) + r_{\text{m0}}^5 \right) \right]^{\frac{1}{5}}, \quad (21)$$

where $\lambda(\beta, r_{\text{mmax}}) = 5C(\beta)/(r_{\text{mmax}}^5 - r_{\text{m0}}^5)$ with $C(\beta)$ given by Eq. (19). Alternatively, we have,

$$\frac{r_{\text{mmax}}^5 - r_{\text{m}}^5}{r_{\text{mmax}}^5 - r_{\text{m0}}^5} = \exp\left(-\frac{5C}{r_{\text{mmax}}^5 - r_{\text{m0}}^5}t\right). \quad (22)$$

Here r_{mmax} is the maximal r_{m} for the agglomeration of Ni particles. The growth of Ni particle is due to the merger of connected neighboring particles. It is plausible to estimate r_{mmax} by allowing the examined particle to absorb all of its connected Ni-particle neighbors. That is, r_{mmax} may be estimated through the following relation:

$$\frac{4\pi}{3}r_{\text{f0}}^3 + \left[\frac{\eta_{\text{Ni}}}{r_{\text{m0}}} / \left(\frac{\eta_{\text{Ni}}}{r_{\text{m0}}} + \frac{\eta_{\text{YSZ}}}{r_{\text{YSZ0}}} \right) \right] \frac{\bar{Z}_0}{2} \left(\frac{4\pi}{3}r_{\text{f0}}^3 + \frac{4\pi}{3}r_{\text{s0}}^3 \right) = \frac{4\pi}{3}r_{\text{lmax}}^3, \quad (23)$$

where $r_{\text{lmax}} = (1 + \beta)r_{\text{mmax}}$. Quite often, the initial Ni and YSZ particles are of similar sizes. Simplifying Eq. (23) with $r_{\text{m0}} = r_{\text{YSZ0}}$ and some simple algebra yields,

$$r_{\text{mmax}} = \left(\frac{\eta_{\text{Ni}}\bar{Z}_0(1 + 3\beta^2) + (1 + \beta)^3}{(1 + \beta)^3} \right)^{\frac{1}{3}} r_{\text{m0}}. \quad (24)$$

The dependence of $r_{\text{mmax}}/r_{\text{m0}}$ on β for the typical case of $\eta_{\text{Ni}} = 0.4$ and $\bar{Z}_0 = 6.7$ [50] is shown in Fig. 4. As may be seen from Fig. 4, $r_{\text{mmax}}/r_{\text{m0}}$ is essentially a constant for $\beta > 0.5$.

With Eq. (24), there is only one adjustable parameter, β , in the theoretical model. For convenience, the two-parameter model and the one-parameter model are named as Model A and Model B, respectively. Fig. 5 shows the comparison of Model B with the experimental data. It is natural to expect that the fitting quality of Model B with only one adjustable parameter is lower than that for Model A. As shown in Fig. 5, however, Model B also fits the experiments very well. The worst fit is seen for Cell A. Nevertheless, the largest fitting error is only 15 nm, or a relative error of 4%, well below the experimental uncertainty. As it is rather difficult to reproduce several different experimental results with just one adjustable parameter, the good fitting quality of Model B is highly satisfactory. Moreover, it is noted that the fittings by Model A and Model B also produce reasonably similar results for the unknown parameters. For example, the values of β determined by Model A/Model B are 0.83/0.76, 0.94/0.94 and 0.75/0.68 for Cell A, Cell B and Cell C, respectively. The corresponding values in μm for r_{mmax} are 0.366/0.383, 1.35/1.35 and 0.404/0.423, respectively. Therefore, Model B is a good reflection of Model A. It is recommendable to use Model B instead of Model A as reducing the number of adjustable parameters is often strongly favorable for a theoretical model.

4. Summary

A theoretical model for surface diffusion driven Ni-particle agglomeration in SOFC anode is proposed. The diffusion process is determined by the Fick's law and the Gibbs–Thomson relation for a system of random packing spherical Ni particles with two

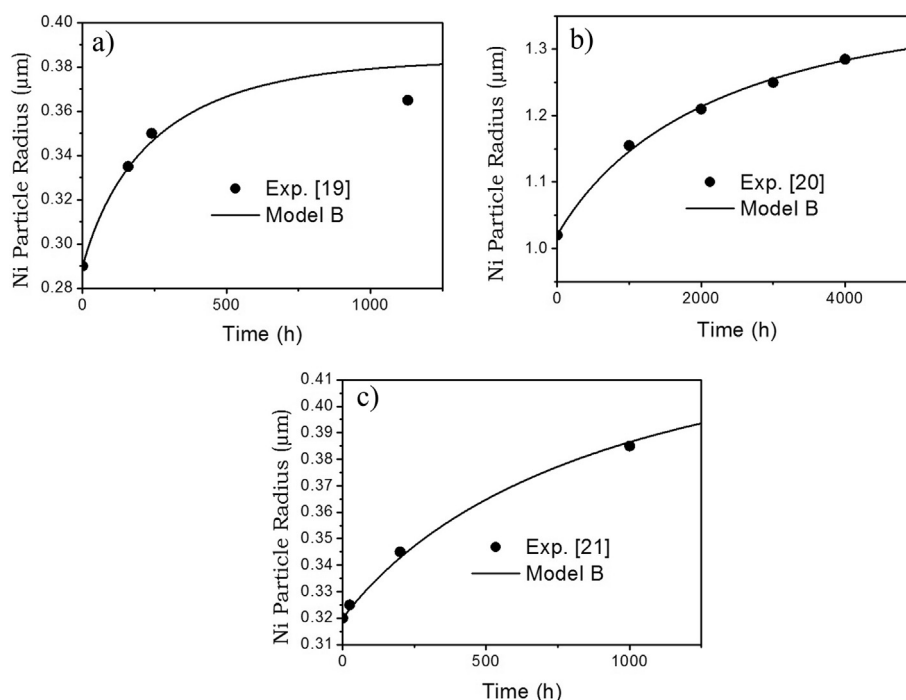


Fig. 5. Fitting of the experimental data by Model B: a) Cell A [19], b) Cell B [20], c) Cell C [21].

representative radii. A lifetime distribution for the Ni-particle growth by the surface diffusion is introduced to account for the statistical connectivity nature of the percolating Ni-particle network confined by the YSZ backbone. The mass diffusion is further quantified through the concept of coordination number in the percolation theory. A simple analytical expression with two adjustable parameters is obtained. The model is shown to be in excellent agreements with the experimental results for different microstructure compositions and operating temperatures. Furthermore, the role of the YSZ backbone on limiting Ni-particle agglomeration is used to estimate the maximal size of Ni particle, yielding a model with only one adjustable parameter. The one-parameter model is also found to agree with the experiments very well, strongly suggesting that the fundamental physics for the Ni-particle growth is well represented in the theory.

Acknowledgments

The financial support of the State Key Development Program for Basic Research of China (973 Grant No. 2012CB215405), the National Natural Science Foundation of China (11374272, J1103207 & 11074233) and the Specialized Research Fund for the Doctoral Program of Higher Education (20113402110038 & 20123402110064) are gratefully acknowledged.

References

- [1] M. Hattori, Y. Takeda, Y. Sakaki, A. Nakanishi, S. Ohara, K. Mukai, J.H. Lee, T. Fukui, *J. Power Sources* 126 (2004) 23–27.
- [2] J. Van Herle, R. Vasquez, *J. Eur. Ceram. Soc.* 24 (2004) 1177–1180.
- [3] C. Haering, A. Roosen, H. Schichl, M. Schnöller, *Solid State Ionics* 176 (2005) 261–268.
- [4] B. Butz, P. Kruse, H. Stormer, D. Gerthsen, A. Müller, A. Weber, E. Ivers-Tiffée, *Solid State Ionics* 177 (2006) 3275–3284.
- [5] W. Coors, J. O'Brien, J. White, *Solid State Ionics* 180 (2009) 246–251.
- [6] A.N. Kumar, B.F. Sørensen, *Mater. Sci. Eng. A* 333 (2002) 380–389.
- [7] Y.C. Hsiao, J.R. Selman, *Solid State Ionics* 98 (1997) 33–38.
- [8] A. Hauch, M. Mogensen, A. Hagen, *Solid State Ionics* 192 (2011) 547–551.
- [9] Z. Yang, K.S. Weil, D.M. Paxton, J.W. Stevenson, *J. Electrochem. Soc.* 150 (2003) A1188.
- [10] D. Larrain, D. Favrat, *J. Power Sources* 161 (2006) 392–403.
- [11] L. Chih-Kuang, C. Tsung-Ting, Y.P. Chyou, C. Lih-Kwang, *J. Power Sources* 164 (2007) 238–251.
- [12] A. Nakajo, Z. Wuillemin, D. Favrat, *J. Power Sources* 193 (2009) 203–215.
- [13] K. Hilpert, D. Das, M. Miller, D. Peck, R. Weiss, *J. Electrochem. Soc.* 143 (1996) 3642.
- [14] M. Stanislawski, E. Wessel, K. Hilpert, T. Markus, L. Singheiser, *J. Electrochem. Soc.* 154 (2007) A295.
- [15] X. Sun, W.N. Liu, E. Stephens, M.A. Khaleel, *J. Power Sources* 176 (2008) 167–174.
- [16] M.J. Jørgensen, P. Holtappels, C. Appel, *J. Appl. Electrochem.* 30 (2000) 411–418.
- [17] Y.L. Liu, A. Hagen, R. Barfod, M. Chen, H.J. Wang, F.W. Poulsen, P.V. Hendriksen, *Solid State Ionics* 180 (2009) 1298–1304.
- [18] J.H. Lee, H. Moon, H.W. Lee, J. Kim, J.D. Kim, K.H. Yoon, *Solid State Ionics* 148 (2002) 15–26.
- [19] A. Faes, A. Hessler-Wyser, D. Presvytes, C.G. Vayenas, J. Van Herle, *Fuel Cells* 9 (2009) 841–851.
- [20] D. Simwonis, F. Tietz, D. Stöver, *Solid State Ionics* 132 (2000) 241–251.
- [21] P. Tanasini, M. Cannarozzo, P. Costamagna, A. Faes, J. Van Herle, A. Hessler-Wyser, C. Comninellis, *Fuel Cells* 9 (2009) 740–752.
- [22] H.S. Song, S.H. Hyun, J. Kim, H.W. Lee, J. Moon, *J. Mater. Chem.* 18 (2008) 1087–1092.
- [23] M. Shah, G. Hughes, P.W. Voorhees, S.A. Barnett, *ECS* 35 (2011) 2045–2053.
- [24] Y.L. Liu, K. Thydén, et al., *Solid State Ionics* 206 (2012) 97–103.
- [25] A. Ioselevich, A. Kornyshev, W. Lehnert, *J. Electrochem. Soc.* 144 (1997) 3010.
- [26] R. Vaßen, D. Simwonis, D. Stöver, *J. Mater. Sci.* 36 (2001) 147–151.
- [27] H.Y. Chen, H.C. Yu, J. Scott Cronin, J.R. Wilson, S.A. Barnett, K. Thornton, *J. Power Sources* 196 (2011) 1333–1337.
- [28] A. Ioselevich, A.A. Kornyshev, W. Lehnert, *Solid State Ionics* 124 (1999) 221–237.
- [29] K. Park, S. Yu, J. Bae, H. Kim, Y. Ko, *Int. J. Hydrogen Energy* 35 (2010) 8670–8677.
- [30] S.P. Simner, M.D. Anderson, M.H. Engelhard, J.W. Stevenson, *Electrochem. Solid-State Lett.* 9 (2006) A478.
- [31] P. Holtappels, J. Bradley, J. Irvine, A. Kaiser, M. Mogensen, *J. Electrochem. Soc.* 148 (2001) A923.
- [32] H. Yokokawa, T. Horita, N. Sakai, K. Yamaji, M. Brito, Y.P. Xiong, H. Kishimoto, *Solid State Ionics* 177 (2006) 3193–3198.
- [33] T. Komatsu, H. Arai, R. Chiba, K. Nozawa, M. Arakawa, K. Sato, *Electrochem. Solid-State Lett.* 9 (2006) A9.
- [34] Y. Matsuzaki, I. Yasuda, *J. Electrochem. Soc.* 148 (2001) A126.
- [35] M.H. Pihlatie, A. Kaiser, M. Mogensen, M. Chen, *Solid State Ionics* 189 (2011) 82–90.
- [36] S. Jiang, *J. Mater. Sci.* 38 (2003) 3775–3782.

- [37] M.H. Pihlatie, H.L. Frandsen, A. Kaiser, M. Mogensen, *J. Power Sources* 193 (2010) 2677–2690.
- [38] A. Nakajo, P. Tanasini, S. Diethelm, J.V. herle, D. Favrat, *J. Electrochem. Soc.* 158 (2011) B1102–B1118.
- [39] D. Chen, Z. Lin, H. Zhu, R.J. Kee, *J. Power Sources* 191 (2009) 240–252.
- [40] Jayant V. Deshpande, Subhash C. Kochar, Harshinder Singh, *J. Appl. Probab.* 23 (1986) 748–758.
- [41] A. Bertei, C. Nicoletta, *J. Power Sources* 196 (2011) 9429–9436.
- [42] A. Baldan, *J. Mater. Sci.* 37 (2002) 2171–2202.
- [43] R. Coble, T. Gupta, Gordon and Breach, New York, 1967, 423.
- [44] S. Georges, G. Parrou, M. Henault, J. Fouletier, *Solid State Ionics* 177 (2006) 2109–2112.
- [45] J.M. Klein, Y. Bultel, S. Georges, M. Pons, *Chem. Eng. Sci.* 62 (2007) 1636–1649.
- [46] M. Suzuki, T. Oshima, *Powder Technol.* 35 (1983) 159–166.
- [47] S. Sunde, *J. Electrochem. Soc.* 143 (1996) 1930–1939.
- [48] P. Costamagna, M. Panizza, G. Cerisola, A. Barbucci, *Electrochim. Acta* 47 (2002) 1079–1089.
- [49] V.M. Janardhanan, V. Heuveline, O. Deutschmann, *J. Power Sources* 178 (2008) 368–372.
- [50] Jay Sanyal, Graham M. Goldin, Huayang Zhu, Robert J. Kee, *J. Power Sources* 195 (2010) 6671–6679.
- [51] M. Chen, T. Liu, Z. Lin, *ECS Electrochem. Lett.* 2 (2013) F82–F84.
- [52] Sun-Dong Kim, et al., *J. Power Sources* 163 (2006) 392–397.
- [53] Trine Klemensø, et al., *J. Power Sources* 195 (2010) 7295–7301.
- [54] L. Holzer, et al., *J. Power Sources* 196 (2011) 1279–1294.